JOURNAL OF MATERIALS SCIENCE 13 (1978) 1957–1970

The plastic deformation behaviour of linear polyethylene and polyoxymethylene

P. D. COATES, I. M. WARD,
Department of Physics, University of Leeds, Leeds, UK

The plastic deformation behaviour of linear polyethylene and polyoxmethylene has been studied as a function of strain rate over a very wide range of plastic strains (deformation ratios up to ~ 25). The results have been examined in terms of the concept of a true stress–strain–strain rate relationship. It has been shown that results for drawn fibres and extruded rods are compatible on this basis, and true stress–strain–strain rate surfaces can be defined. The significance of these results with regard to both tensile drawing and hydrostatic extrusion processes is considered. A preliminary discussion of the rate dependence is also presented.

1. Introduction

There has been a considerable revival of interest in the tensile drawing behaviour of such crystalline polymers as linear polyethylene (LPE) [1–8], polyoxymethylene (POM) [9] and polypropylene [10], due to the possibility of obtaining ultra-high stiffness materials in this way. Very high draw ratios (e.g. $\lambda \sim 30$) have been attained in LPE and POM, representing a region of strain not previously investigated for solid polymers. The present work is concerned with the plastic deformation of two polymers, LPE and POM, over a wide range of strain, from $\epsilon = 0$ ($\lambda = 1$) to $\epsilon = 3.2$ ($\lambda \sim 25$), at elevated temperatures.

These polymers neck and cold-draw. Once the neck has formed the deformation is inhomogeneous and there is a non-uniform distribution of stress and strain along the length of the specimen. Following Nadai [11] and Orowan [12], the discussion of such behaviour in metals is usually in terms of the true stress–strain curve [13]. A complicating factor in the case of polymers is that the mechanical behaviour is very dependent on strain rate (or time) and temperature. Vincent [14, 15] has developed the concept of the true stress–strain curve to deal with both necking and failure in polymers. In the latter case, fracture was assumed to be defined by a stress/strain/time/temperature map. Following these ideas we assume that for a given temperature and strain rate there is a unique relationship between true stress and strain. Looked at another way, it is assumed that at a fixed temperature the strain determines the relationship between true stress and strain rate. We are dealing here with plastic strain rate, and therefore the stress we are considering is that stress required to deform the material plastically at a given strain rate, i.e. the true stress is the flow stress of the Eyring-type formulation for plastic deformation.

It has been established that for a given set of drawing conditions the structure and properties of LPE are uniquely related to the draw ratio for a given chemical composition and initial morphology, provided that suitable drawing conditions are satisfied [1–8]. This suggests that it is reasonable to expect the mechanical behaviour (e.g. the relationship between stress and strain rate at a fixed temperature) to relate uniquely to the strain, irrespective of the history of deformation.

Such an assumption might appear to be too sweeping a simplification, in view of the complex viscoelastic behaviour of polymers. We are, however, dealing with a very large range of plastic strain in these polymers, corresponding to extension ratios up to 25. The structure and properties are also changing dramatically with strain, as exemplified by the change in Young's modulus by a factor of about thirty for polyethylene. We are therefore attempting to develop an overall view, ignoring the undoubted complexities

which are apparent if the viscoelastic behaviour is considered in detail at any stage in the deformation.

A principal aim of the work described in this paper is to determine the true stress–strain–strain rate relationships for each polymer under given conditions such as temperature, pressure, and the initial thermal treatment of the specimen. We will discuss how this information is vital to the understanding of practical deformation processes such as drawing and hydrostatic extrusion. In fact, Takayanagi and co-workers [16, 22–24] have implicitly assumed the existence of a true stress–strain curve for a polymer in their attempts to analyse the hydrostatic extrusion process, but without recognizing the importance of strain rate and the major influence of the degree of plastic strain on the strain rate dependence.

The existence of a unique true stress–strain–strain rate surface implies that any deformation process can be considered as taking an element of material on a specific path across this surface. Once determined, the true stress–strain–strain rate relationships enable a quantitative examination of the viability of a given polymeric material in any practical deformation process.

The results obtained here also have interesting implications regarding the mechanisms of plastic deformation when examined from the viewpoint of an activated site theory. An indication of this will be given here, but the main discussion will be made in a separate publication.

2. Materials

Two crystalline polymers have been investigated:

(i) Linear polyethylene (LPE) grade Rigidex 50 (R50), $\bar{M}_w = 101\,450$, $\bar{M}_n = 6180$, which was supplied in pellet form by BP Chemicals International Ltd.

(ii) Polyoxymethylene (POM) grades Delrin 500 (D500), $\bar{M}_w = 90\,000$, $\bar{M}_n = 45\,000$, and Delrin 150 (D150); $\bar{M}_w = 120\,000$, $\bar{M}_n = 60\,000$, made by Du Pont de Nemours, and obtained commercially in pellet or rod form.

3. The determination of true stress–strain–strain rate data

As discussed above, the formation of a neck in tensile drawing leads to a non-uniform distribution of stress and strain in the specimen. This makes it difficult to obtain true stress–strain–strain rate data over the whole range of strains from straightforward tensile tests. The neck is a region of inhomogeneous drawing, in which the strain and strain rate cannot be varied independently. For this reason only limited use can be made of specimens which deform through a neck, and we have circumvented the problem by performing separate drawing experiments. Three regions of strain have been covered: first, the low strain region (from isotropic to deformation ratios (R) up to ~ 5) covering strain values normally encountered only in the neck region (Fig. 1), secondly the intermediate strain region ($R \sim 5$ to ~ 15) covering strain values encountered partly in the neck region and partly in the post-neck region (Fig. 1), and thirdly the high strain region (draw ratios up to ~ 25), covering strain values which are present only in the post-neck region.

The low strain region involved drawing isotropic material and hydrostatically extruded specimens of low deformation ratio to their initial yield point. In this case, where there is a yield point, we assume that the deformation is homogeneous up to the yield point, and that the latter

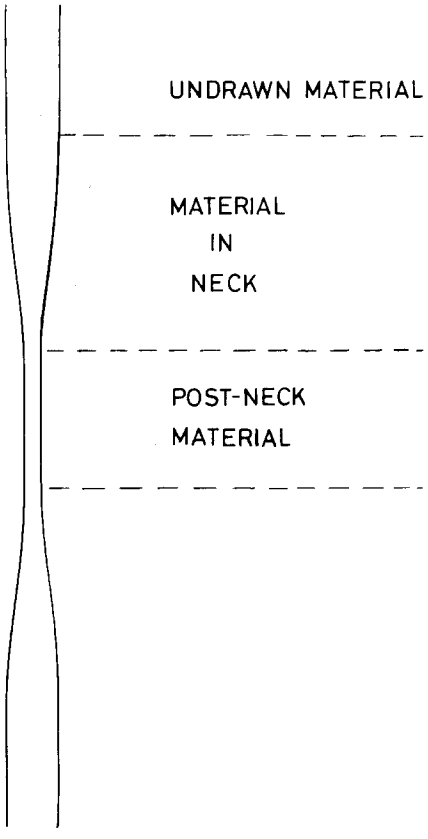

Figure 1 Terms used to describe regions in a drawn sample.

corresponds to the situation where the plastic strain rate in the specimen is identically equal to the extension rate imposed by the tensile testing machine. We can therefore define precisely the relationship between stress and strain rate at the instant where there is zero slope on the load–elongation curve. This stress is conventionally termed the yield stress, σ_y.

The intermediate strain region involved drawing hydrostatically extruded rods of deformation ratio greater than ~5. These samples generally did not exhibit a sharp fall in load at the onset of plastic deformation. Instead the load rose to a roughly constant value, falling slightly with increasing elongation. The yield stress, i.e. that stress which is required to initiate plastic deformation of the sample at a given strain rate and temperature, was therefore determined from the maximum load. At yield, the plastic strain rate in the specimen is equal to the extension rate imposed by the machine, as in the low strain region.

The high strain region involved redrawing fibres which had been predrawn to a draw ratio just beyond that obtained through the neck. In this region the deformation is homogeneous since it consists of drawing material which has passed through the neck. It is, of course, this extra drawing which gives rise to the very high draw ratios and ultra-high modulus material. In this region the stress, strain and strain rate in the material can be defined purely from geometrical consideration, knowing the load at any given instant.

3.1. Low strain region (yield point measurements)

Cylindrical isotropic rods were machined to a chosen gauge length, and had screw-threaded ends. These specimens were then drawn to their yield point in an Instron air oven at a temperature T_d (164° C for POM, and 100° C for LPE) at a constant elongation rate, v cm min^{-1}. At the yield point, the specimen strain rate, $\dot{\epsilon}_y$, corresponds to the machine strain rate, i.e.

$$\dot{\epsilon}_y = v/L$$

where v = elongation rate and L = specimen gauge length. The yield stress, σ_y can be calculated from the load at yield and the original specimen cross-sectional area. The strain at yield, ϵ_y, is very small ($\simeq 0.1$) compared to the range of strain to be covered in the whole work, so we set $\epsilon_y = 0$ (or the draw ratio at yield, $\lambda_y = 1$). The strain rate at yield was varied by altering the cross-head speed, v, or the gauge length, L. The range of strain rate covered in yield point determinations was $\sim 5 \times 10^{-4}$ sec^{-1} to $\sim 10^{-1}$ sec^{-1}.

To obtain data for the strain levels which would normally occur in the neck region in a tensile test, samples were machined from $\frac{1}{2}$ in. diameter hydrostatically extruded rods of LPE [17] and POM [18], to similar dimensions to those used for isotropic material. Alternatively, small diameter extrudates (~1.8 mm and 2.5 mm diameter) were gripped by pin chucks without any machining. In hydrostatic extrusion the actual deformation ratio, R_A, obtained for an isotropic billet of initial diameter d_0, assuming conservation of volume in plastic deformation is $R_A = (d_0/d_p)^2$ where d_p is the extrudate diameter. R_A can be equated to the draw ratio, λ, referred to in tensile deformation. Large scale extrudates of extrusion ratio $R_A = 1.5$ to $R_A = 5$ and smaller scale extrudates up to $R_A = 5$ were drawn to their yield point as described for isotropic material. Thus the yield stress at strain $\epsilon = \ln R_A$ and strain rate $\dot{\epsilon} = v/L$ was determined. The small increase in strain associated with reaching the yield point of the extrudate is negligible, compared to the initial extrudate strain, $\ln R_A$.

3.2. Intermediate strain region (yield point measurements)

An overlap in data is required for tests on materials in the range of strain normally encountered in the neck region and tests on materials in the range of strain encountered in the post neck region, i.e. in the region of deformation ratio between ~6 and 15.

It was possible to measure the yield stress of extruded LPE and POM samples up to $R_A \simeq 9$ by the technique described above for the lower strain samples. In the case of POM this range of strain could not be extended significantly, due to the limited range of extrusion ratio [18].

In the case of LPE, drawing of small scale extrudates of deformation ratios greater than ~9 by the above method proved to be unreliable, due to slipping at the grips. Large diameter extruded samples were not available for this range of extrusion ratio. Therefore, in order to obtain yield stress data for deformation ratios greater than ~9, small scale extrudates were drawn on an Instron tensile testing machine using a gauge length defined by a temperature profile. The experimental

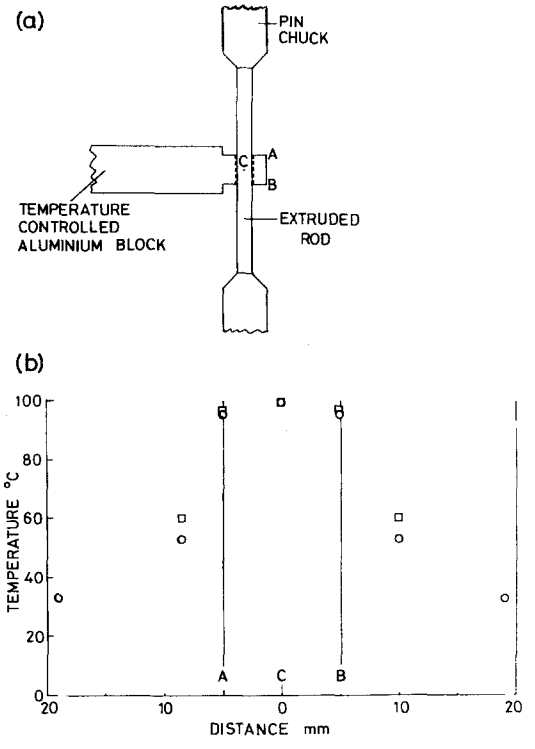

Figure 2 Drawing extrudates using a gauge length defined by a temperature profile: (a) experimental arrangement (b) temperature profile along sample, □ at centre of specimen, ○ at surface of specimen.

arrangement is shown in Fig. 2a. The specimen passed through a hole in a temperature-controlled aluminium block. The nominal gauge length, AB, was 10.0 mm. The surface temperature of the sample was monitored by a thermocouple inserted through the aluminium block at C. When the gauge length portion of the sample had reached equilibrium at 100° C, it was drawn at a chosen extension rate. The clamped material stayed at ambient temperature, ensuring sufficiently large gripping forces for drawing to proceed. The yield stress and strain rate were therefore obtained at a strain $\ln R_A$.

The measured temperature profile is shown in Fig.2b. The small temperature gradient along the gauge length, together with the steep temperature gradient away from the gauge length, suggest that the errors are small when using the set value of 10 mm for the gauge length in calculation of the strain rate at yield. In subsidiary experiments gauge marks at 1 mm intervals along the specimen showed that drawing only occurred in the gauge length region.

3.3. High strain region (redrawing experiments)

This section deals with obtaining data for draw ratios greater than ~8, up to ~25. Although it is possible to obtain true stress–strain–strain rate data from post-neck material in a drawn specimen, the measurements tend to be uncertain in the presence of the neck due to non-uniformity of strain. Also material may draw out from the clamp region when the neck has fully propagated along the specimen. The central portion of a drawn sample could be removed and redrawn to obviate these problems, but a more convenient method is the redrawing of continuously drawn fibres. Melt spun filaments of each polymer were first drawn continuously over a heated pin to a draw ratio, λ, just beyond that produced through the neck in a tensile drawing process. The value of λ for LPE was 10.6, and for POM, 7.2. The drawing temperature for each polymer was the maximum drawing temperature to be employed in any subsequent redrawing process, namely 100° C for LPE and 164° C for POM.

Each specimen to be redrawn had gauge marks at 1 mm intervals over the whole gauge length and was mounted on a card holder. This assembly was mounted in clamps in an Instron air oven, with the specimen ends passing completely through the clamps. Redrawing was then performed at the original temperatures of 100° C for LPE and 164° C for POM. In addition some redrawing was carried out at 72° C and 84° C for LPE. Although these materials do not fall within our original definition of the true stress–strain–strain rate relationship which applied for deformation at a single fixed temperature, it will be shown that the results are of considerable interest.

Since the specimens in this group consisted entirely of "post-neck" material, the redrawing process was macroscopically homogeneous. This was confirmed by careful measurements on redrawn specimens which showed that originally cylindrical specimens become longer thinner cylinders and the originally uniformly spaced gauge marks remain uniformly spaced. This type of deformation therefore allows a simple simultaneous evaluation of true stress, strain and strain rate.

Consider macroscopically homogeneous redrawing of a cylindrical specimen originally at draw ratio λ_1, at a constant elongation rate

v cm min^{-1}. After t sec drawing the sample length is

$$L_t = L_0 + e_t$$

where L_0 = original gauge length at time $t = 0$ and e_t = elongation at time t. The draw ratio at time t in the redrawing process is

$$\lambda_t = \frac{L_t}{L_0} = 1 + \frac{e_t}{L_0} \tag{3.1}$$

The total draw ratio of the sample at time t therefor is

$$\lambda_{TOT} = \lambda_1 \lambda_t \tag{3.2}$$

and the total strain at time t,

$$\epsilon_{TOT} = \ln(\lambda_{TOT}).$$

For constant elongation rate, $de_t/dt = v =$ constant, and so

$$\frac{d\lambda_{TOT}}{dt} = \frac{\lambda_1}{L_0}\frac{de_t}{dt} = \frac{\lambda_1 v}{L_0} = \text{constant} \tag{3.3}$$

i.e. the draw ratio increases linearly with time. The total strain rate at time t is

$$\dot{\epsilon}_t = \frac{d\epsilon_{TOT}}{dt} = \frac{d}{dt}(\ln \lambda_{TOT}) = \frac{1}{\lambda_{TOT}}\frac{d\lambda_{TOT}}{dt} \tag{3.4}$$

since the total strain $\epsilon_{TOT} = \ln(\lambda_{TOT})$; i.e. the total strain rate decreases during the tensile test, and is inversely proportional to the draw ratio.

The cross-sectional area of the specimen at time t, assuming conservation of volume in plastic deformation, is

$$A_t = A_0 \frac{L_0}{L_t} = \frac{A_0}{\lambda_t} = A_0 \frac{\lambda_1}{\lambda_{TOT}}, \tag{3.5}$$

i.e. the cross-sectional area is inversely proportional to the draw ratio.

The drawing load and therefore the drawing force, F, is monitored with drawing time, so the drawing stress at time t, is given by

$$\sigma_t = F_t/A_t. \tag{3.6}$$

Thus simultaneous sets of values for σ_t, ϵ_{TOT} (or λ_{TOT}) and $\dot{\epsilon}_t$ can be obtained from Equations 3.6, 3.2 and 3.4, e.g. by choosing values of λ_{TOT} and calculating values for σ_t and $\dot{\epsilon}_t$. Choice of elongation rate (v) initial gauge length (L_0) and initial draw ratio (λ_1) allow a range of strain rate to be investigated. In the present work, initial gauge lengths between 1 cm and 5 cm were employed, and the range of strain rate covered was $\sim 10^{-4}$ sec^{-1} to $\sim 10^{-1}$ sec^{-1}.

4. Measurement of Young's modulus on redrawn fibres

As discussed above, if the concept of a unique stress–strain–strain rate relationship is valid, the strain rate path followed in obtaining a particular draw ratio should not influence the drawn product. Samples of given initial thermal treatment can then be defined by their draw ratio alone. In the studies of the drawing behaviour of these materials [1, 2, 5, 8] it has been shown that polymers of given molecular weight characteristics and initial thermal treatment will be identical in structure and properties for a given draw ratio, providing that the drawing process has achieved its limiting

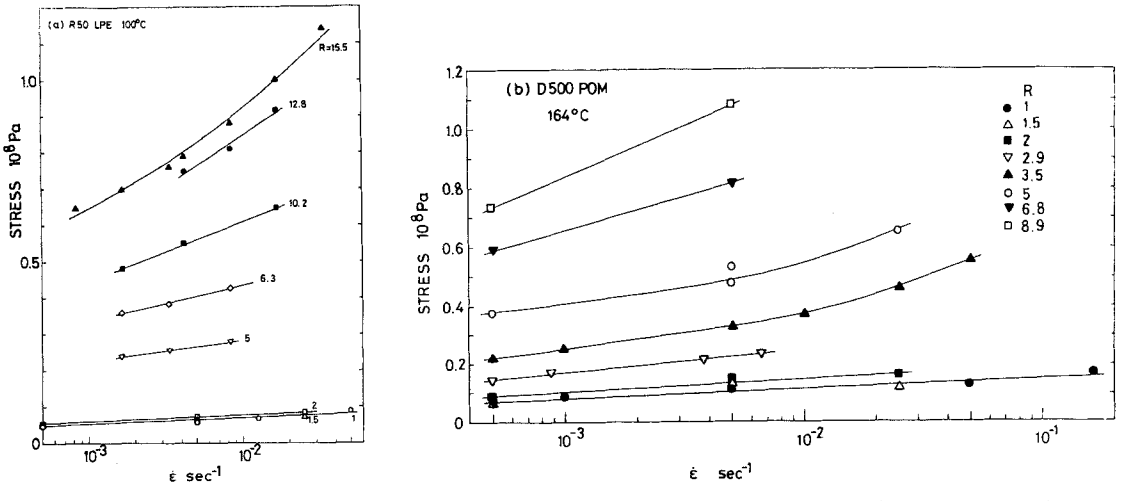

Figure 3 Strain rate dependence of the yield stress of isotropic ($R = 1$) and hydrostatically extruded samples of (a) Rigidex 50 LPE at 100° C, (b) Delrin 500 POM at 164° C.

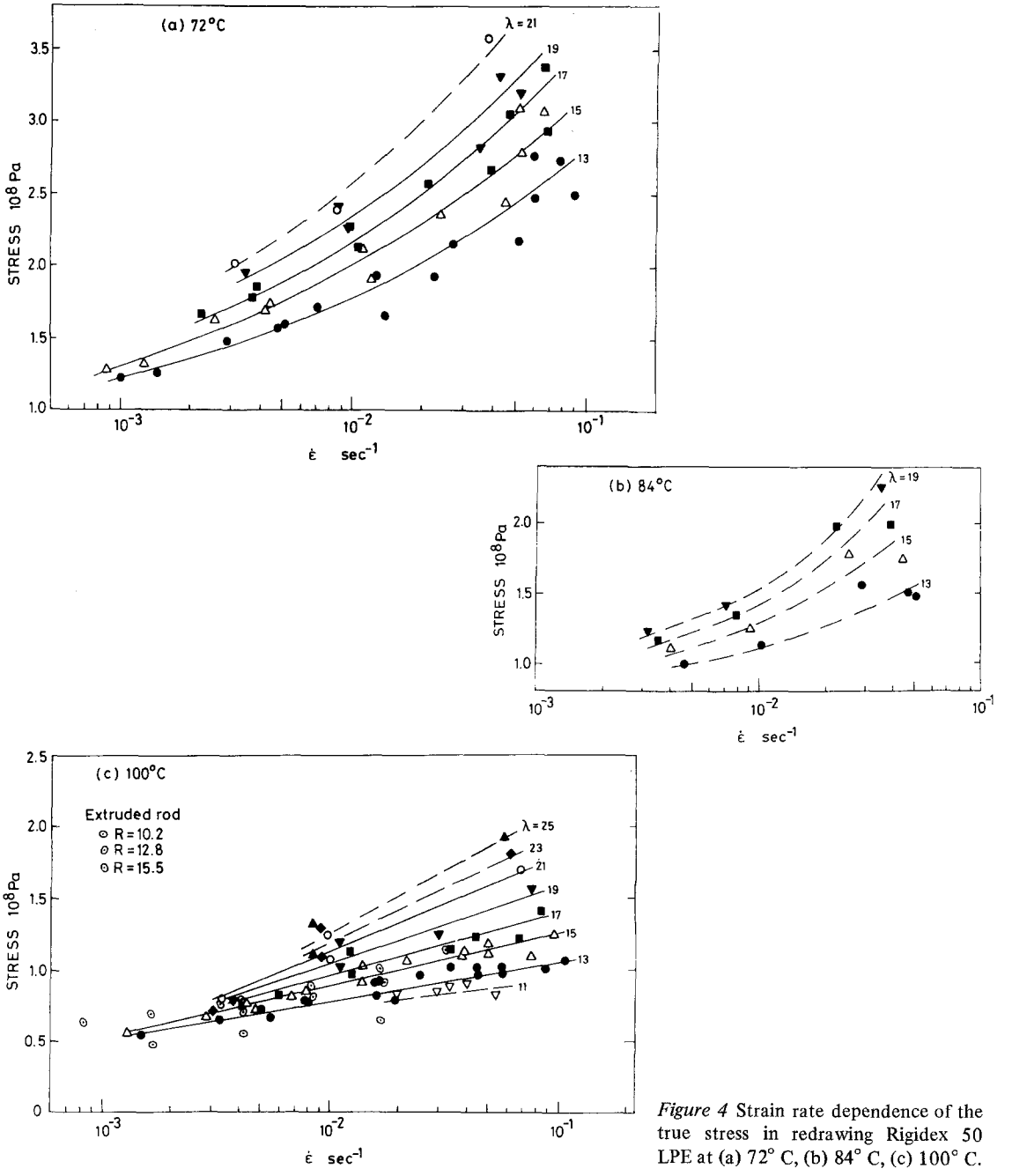

Figure 4 Strain rate dependence of the true stress in redrawing Rigidex 50 LPE at (a) 72° C, (b) 84° C, (c) 100° C.

effectiveness with regard to increasing the degree of alignment of the material. It has further been established that the Young's modulus of the drawn material is a good operational guide to the effectiveness of the drawing procedure. We have therefore used Young's modulus measurements to examine whether there are any significant differences between final products obtained by different strain rate paths. As in previous work [1, 2, 5, 8] the room temperature Young's modulus was obtained from 10 sec isochronal stress–strain curves constructed from the dead loading creep response, at a reference strain of 0.1%.

5. Results

Data obtained from yield stress measurements on isotropic and extruded samples are shown in Fig. 3a for LPE at 100° C and Fig. 3b for POM at 164° C. The stress–strain rate relationship is roughly linear for LPE in the range of strain and

strain rate covered, but shows evidence of non-linearity at quite low deformation ratios in the case of POM. However, the amount of data and the range of strain rates covered are both limited, due to a limited number of extruded samples being available.

True stress values obtained from redrawing fibres are plotted against true strain rate for constant values of overall draw ratio, λ_{TOT}, in Fig. 4 for LPE and in Fig. 5 for POM. In general the flow stress–strain rate relationship is non-linear for both polymers. The strain hardening behaviour of LPE increases with decreasing temperature. The higher molecular weight grade of POM (D150) exhibits a greater degree of strain hardening than the lower molecular weight grade at the same temperature.

It was possible to obtain a good overlap in the range of strain covered by the intermediate and high strain experiments in the case of LPE at 100° C. Data from LPE yield point measurements at 100° C are included in Fig. 4c, showing the excellent agreement in results. Only a very small amount of overlapping data could be obtained for D500 POM at 164° C (Fig. 5a) due to a limited amount of samples, but again the agreement between yield point measurements and redrawing is within experimental error.

True stress–strain relationships can be obtained by taking constant strain rate sections through the stress versus strain rate curves. Figs. 6 and 7 show true stress–strain curves for R50 LPE at 100° C and D500 POM at 164° C respectively, for deformation ratios from 1 to 25. These curves are a

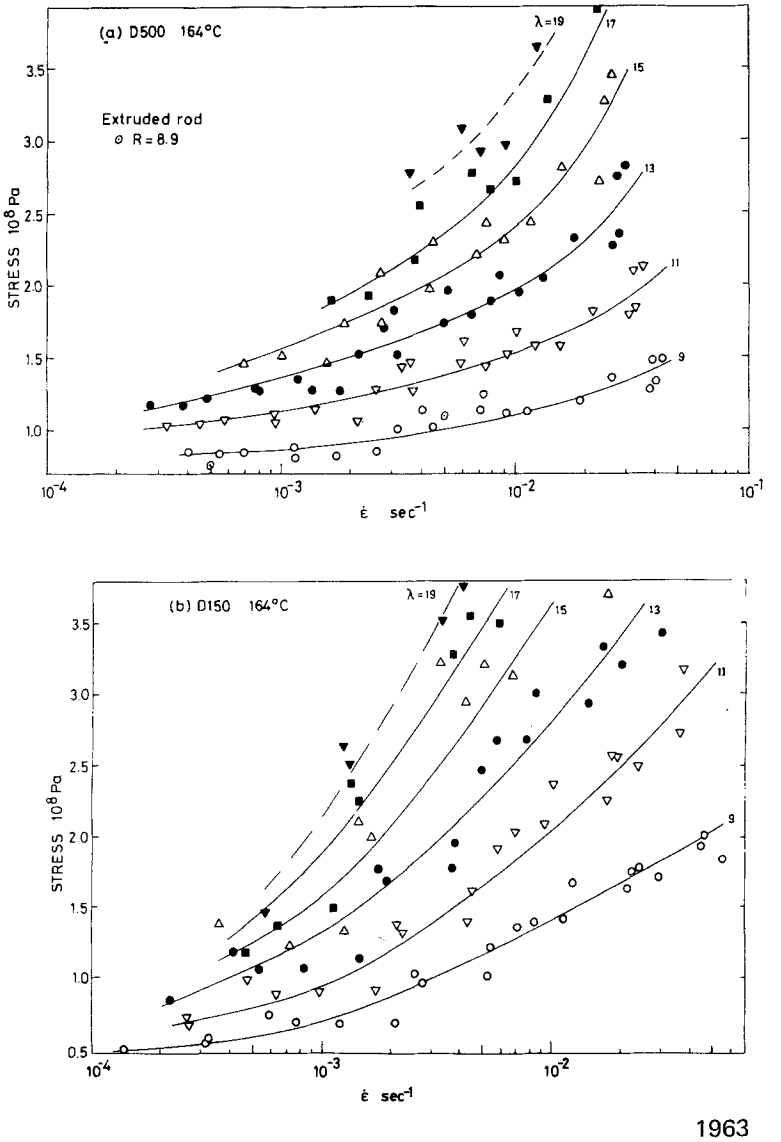

Figure 5 Strain rate dependence of the true stress in redrawing (a) Delrin 500 POM at 164° C and (b) Delrin 150 POM at 164° C.

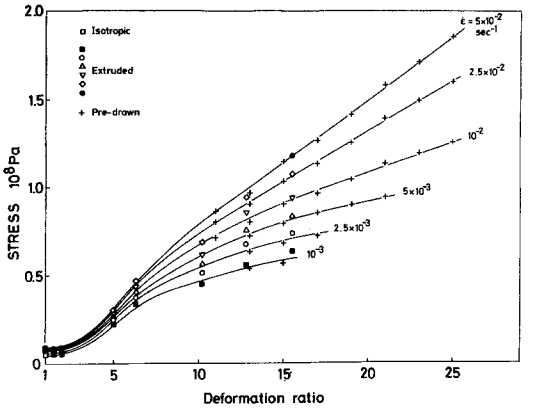

Figure 6 True stress–deformation ratio–strain rate relationships for Rigidex 50 LPE at 100° C.

two-dimensional representation of the flow stress surface for each polymer at the given drawing temperature and initial morphology. Representations of this surface for R50 LPE and D500 POM are shown in Fig. 8. A notable feature of the flow stress–strain curves is the very marked dependence of the flow stress not only on strain but also on strain rate at high strains.

The Young's modulus–draw ratio results for LPE are shown in Fig. 9 and those for POM in Fig. 10, for samples drawn at various elongation rates.

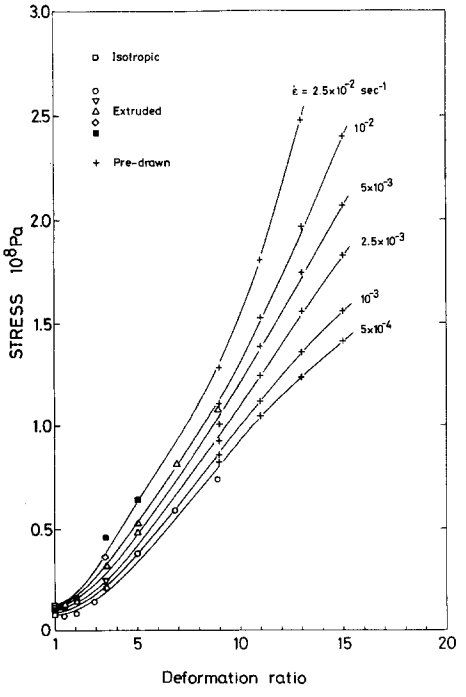

Figure 7 True stress–deformation ratio–strain rate relationships for Delrin 500 POM at 164° C.

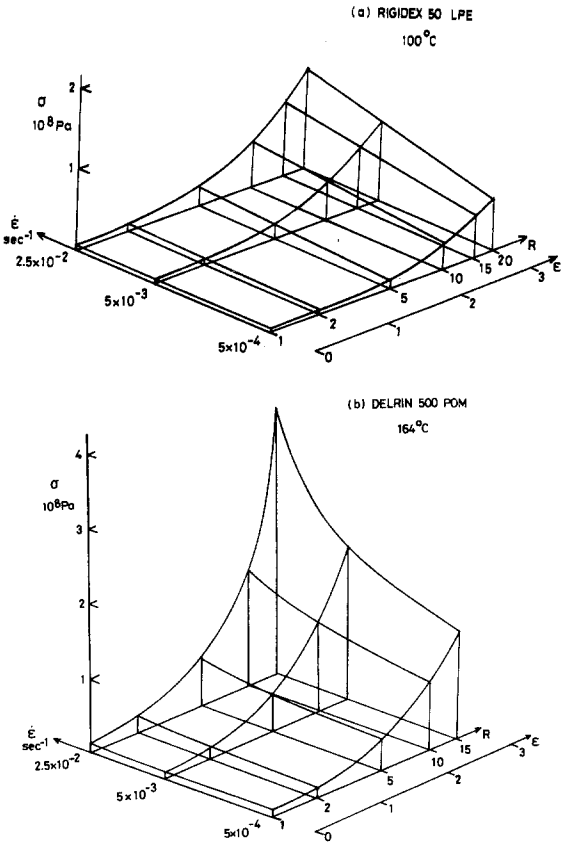

Figure 8 True stress–strain–strain rate surfaces for (a) Rigidex 50 LPE at 100° C and (b) Delrin 500 POM at 164° C.

The LPE modulus values lie on two lines, for redrawing at 100° C and 72° C respectively. No effect of elongation rate could be discerned. Both D500 and D150 POM modulus values lie on the same curve, and again no effect of elongation rate could be discerned.

6. Discussion

6.1. True stress–strain–strain rate surface

The drawing experiments described above were performed to determine the true stress–strain–strain rate surface for each polymer at the quoted temperatures. The data obtained from the drawing of isotropic and extruded samples to their yield point, and from the redrawing of fibres are in good agreement in the range of draw ratios where some overlap between the two tests is possible (Figs. 4 and 5). This agreement between two distinct tests supports the concept of a true flow stress surface.

Further supporting evidence comes from investigations of the rate dependence of the flow stress of LPE by Davis and Pampillo [19, 20]. In an

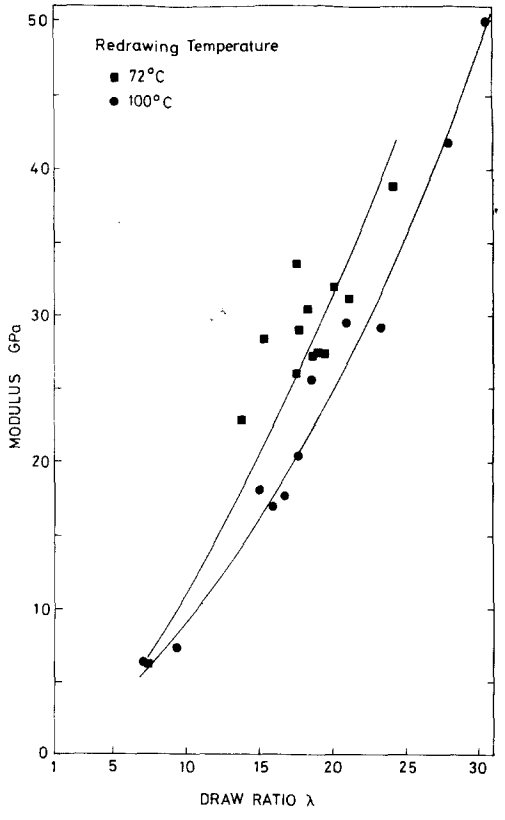

Figure 9 Room temperature Young's modulus versus draw ratio for Rigidex 50 LPE redrawn at 100° C and 72° C at various elongation rates.

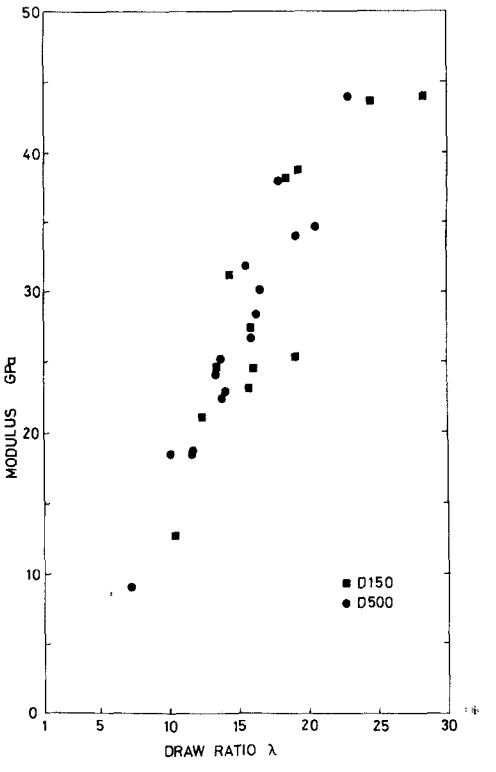

Figure 10 Room temperature Young's modulus versus draw ratio for Delrin 500 POM and Delrin 150 POM, both redrawn at 164° C at various elongation rates.

attempt to ensure that the polymer had the same structure for each stress measurement, Davis and Pampillo initially performed drawing experiments which involved a jump in strain rate [19], in preference to deforming two different samples at different strain rates. They later used the strain level to define their samples [20]. Also, Wu and Turner [21], working on the same material as Davis and Pampillo, performed strain rate jump tests and found that the flow stress shifted to value corresponding to the stress–strain curve at the new strain rate. They then used stress–strain curve data rather than strain rate jump tests.

The modulus results for both LPE and POM showed no strain rate path dependence, confirming that the strain level attained will define the material produced from a given starting material, at a given drawing temperature. Our modulus measurements thus support the findings of these previous workers and we conclude that true stress data can sensibly be obtained from continuous experiments, and from true stress–strain curves since samples at the same strain level appear to be equivalent in terms of their Young's modulus, regardless of the strain rate path followed.

It should perhaps be emphasized that although the Young's modulus versus draw ratio relationships are independent of strain rate path it is not necessarily implied that all LPE and POM samples of identical draw ratio possess the same structure, or have identical properties. Our other investigations [27] have shown clearly that different initial LPE samples (for example different molecular weight materials) may possess very similar values of Young's modulus for a given draw ratio, but that other properties such as melting point and creep behaviour are different, reflecting different structures. Thus in terms of our philosophy, each polymer of given chemical composition and initial morphology possesses its own unique set of true stress–strain–strain rate relationships. Consideration of the drawing behaviour of, for example, different molecular weight grades of LPE would require a set of true stress–strain–strain rate

relationships for each grade. Knowledge of such relationships for any polymer can provide a firm base for understanding its processing possibilities.

6.2. Tensile deformation processes

A major implication of our findings is that data collected in a uniaxial tensile test can be employed in analysing any predominantly tensile deformation process, at the same temperature. This is an assumption which has been employed, though not stated, by workers attempting to analyse such deformation processes as the flow of a solid polymer through a convergent die (as in extrusion) by using tensile stress–strain data [22–24]. The importance of a unique flow stress surface in this case is that any tensile deformation process at the given temperature will be represented by a specific process flow stress path across the surface. This leads to a further important requirement – that we know, or can obtain, a strain rate field for the deformation process. This is particularly important for crystalline polymers such as LPE and POM since the flow stress depends very strongly on both strain and strain rate, as shown above, whereas it is not of great importance for comparatively non-strain hardening materials (such as metals) where the strain rate dependence of the flow stress is considerably lower.

To illustrate this point, consider the cases of a uniaxial tensile test and hydrostatic extrusion for a crystalline polymer such as LPE or POM. In the uniaxial tensile test the variation of strain rate with position in the specimen is complex, in the presence of a neck. On formation of a neck, polymers often exhibit a load drop, which may or may not involve a drop in true stress, depending upon the relative rates at which the applied load and cross-sectional area are decreasing. In the neck region, where the polymer structure is being drastically reorganized, the strain rate will rise sharply at low draw ratios to some maximum value greater than the imposed machine strain rate. This could be an indication of strain softening, depending upon the way in which the true stress varies. As the neck stabilizes and moves along the specimen the strain rate decreases with increasing draw ratio, and simultaneously the true stress increases (or possibly remains constant), indicating strain hardening. If the post neck region of the sample deforms homogeneously, the strain rate in this region will be inversely proportional to the draw ratio. A schematic representation of the variation

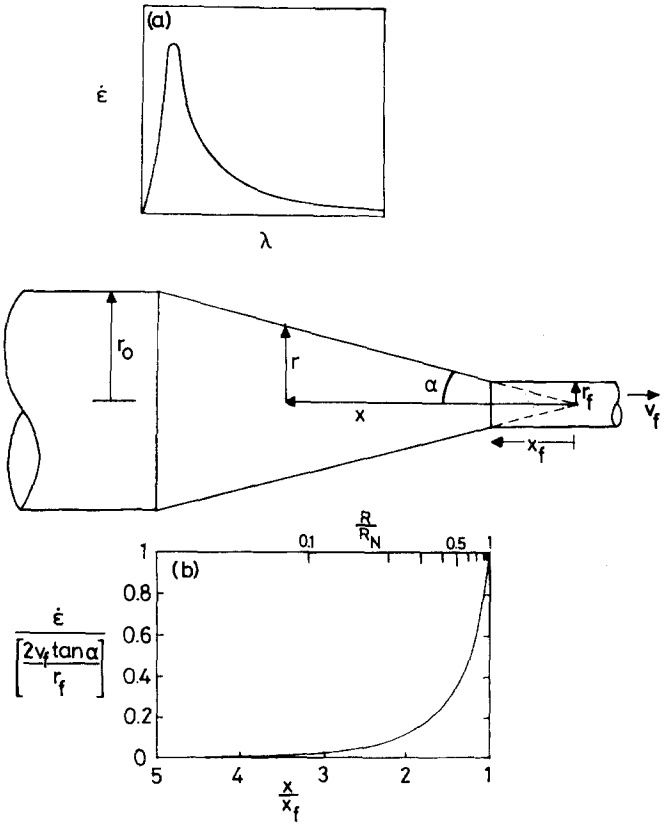

Figure 11 Variation of strain rate with strain in predominantly tensile deformation processes: (a) uniaxial tensile test (schematic), (b) hydrostatic extrusion through conical dies of small semi-angle, α.

of strain rate with draw ratio for an element in a uniaxial tensile specimen is shown in Fig. 11a. The process flow stress path for a uniaxial tensile test at constant elongation rate could thus be depicted as a path across the flow stress surface which follows the strain rate versus draw ratio contour described above.

In the case of hydrostatic extrusion (or ram extrusion) through convergent conical dies, the axial strain rate field is fixed geometrically, and can be calculated [25], for small die cone semi-angles, α, as

$$\dot{\epsilon}_x = 2\frac{v_f r_f^2}{x^3 \tan^2 \alpha}$$

$$\text{or} \quad \dot{\epsilon}_x = 2\frac{v_f}{r_f}\left(\frac{R}{R_N}\right)^{3/2} \tan \alpha$$

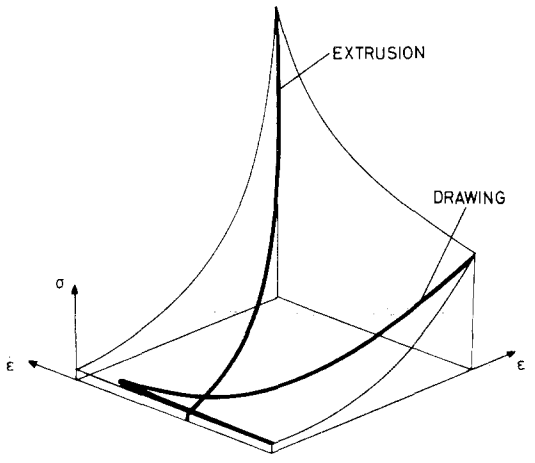

Figure 12 Schematic diagram of process flow stress paths for elements of material undergoing extrusion through a conical die of small semi-angle, and a uniaxial tensile test.

In this expression v_f is the extrudate velocity and r_f is the die exit radius, R is the deformation ratio of material in the die region at a distance x from the die cone apex, and corresponds to the draw ratio λ in a tensile test, for plastic deformation at constant volume. R_N is the nominal deformation ratio, such that

$$R_N = \frac{\text{initial cross-sectional area of billet}}{\text{cross-sectional area of product}}.$$

Inspection of these equations shows that the strain rate increases with increasing deformation ratio, as shown in Fig. 9b. This is clearly a very different – virtually opposite – situation to that encountered in the uniaxial tensile test. The process flow stress path for extrusion will therefore be considerably different from that for uniaxial drawing due to the different strain rate regimes, a fact which has to be accounted for in analysing such a method of deformation. Extrusion through conical dies and uniaxial drawing can therefore be represented by specific, but distinctly different, paths across the true stress–strain–strain rate surface, as shown schematically in Fig. 12.

6.3. Drawing behaviour

It is of interest to consider the factors which affect the tensile drawing of polymers in the light of present and previous work in this department. Studies of the drawing process [1–8] have been previously concerned with the effects of initial morphology, molecular weight and drawing temperature, in determining optimum drawing conditions for the attainment of highly improved properties, such as axial stiffness and creep response.

These experiments were carried out using an Instron tensile testing machine at a constant crosshead speed for various times to impose an overall deformation on the specimen. The specimen is then removed from the testing machine and the maximum draw ratio measured, i.e. the draw ratio in the part of the specimen which has suffered the greatest deformation. In general, the maximum draw ratio increases with the overall deformation, i.e. the maximum draw ratio increases with time. Large differences in the rate at which the maximum draw ratio increases with time can be observed between specimens of different molecular weight and initial morphology. In particular low molecular weight materials show the largest maximum draw ratio after a given time, i.e. there is the largest discrepancy between the overall imposed deformation and the maximum draw ratio. In other words, for these samples the drawing process is most inhomogeneous. This in turn implies that the influence of initial morphology and molecular weight must be seen only in the neck region in this sort of test. It is, of course, also true that the initial composition of the polymer could affect the homogeneous drawing process, but this would appear from the quantitative inter-relationships between stress, strain and strain rate rather than from the draw ratio versus time plots which are only a measure of the inhomogeneous nature of the drawing process.

In order to reach a fuller understanding, and possibly control, of the overall drawing process a more detailed investigation of the neck profile and the effect on the neck of the several variables in drawing is required.

6.4. Effective drawing

The drawing process is a route for producing polymeric materials with enhanced properties, such as higher Young's moduli and improved creep behaviour. It has been shown [1, 2, 5, 8] that the 10 sec tensile modulus of LPE is a unique function of draw ratio, independent of molecular weight and initial sample morphology, for a particular drawing temperature. However, the present investigation, together with other work in this department [26] has shown that drawing at different temperatures does *not* lead to a unique 10 sec tensile modulus–draw ratio relationship. From the present results (Fig. 9) it can be seen that redrawing R50 LPE at 72° C produces a higher modulus at a given draw ratio than redrawing at 100° C. It is also noted that drawing at 72° C involves a greater dependence of the flow stress on strain and strain rate (Fig. 4). It is not clear at present if these two observations are related to the same structural features at the respective drawing temperatures. Deformation at 72° C might involve sliding of larger blocks of crystalline material than at the higher temperature. This could result in a greater crystal continuity, and therefore possibly, a higher 10 sec modulus. Material drawn at 100° C may recrystallize whilst drawing proceeds, so exhibiting a low degree of strain hardening. Molecular chains may slide over each other with less hindrance than at the lower temperature, resulting in the sample having a particular draw ratio but possessing inferior properties to a sample of the same draw ratio produced at the lower temperature. Higher drawing temperatures would involve more viscous flow, less strain hardening, a greater degree of recrystallization and a lower tensile modulus.

The 10 sec modulus is only one aspect of the creep response: the long term creep behaviour is probably a better way of evaluating the effectiveness of a drawing route in producing enhanced properties. It is interesting to speculate here that the creep behaviour of drawn fibres may depend upon their thermal history, notably the drawing temperature, since the 10 sec modulus depends upon the drawing temperature. As yet, however, we do not have detailed evidence that drawing by a higher strain hardening route produces material with superior creep behaviour.

A further important parameter to be considered in the present discussion is molecular weight. Work in this laboratory [27] has shown that LPE samples of different molecular weights drawn to the same draw ratio at a fixed temperature have the same 10 sec tensile modulus, but different long term creep responses. This result again suggests that the long term creep behaviour is a more sensitive parameter for evaluating the drawing process than the 10 sec modulus, although the latter remains a useful guide.

The LPE samples showing the best creep behaviour also appear to exhibit the greatest strain hardening at a fixed drawing temperature, although quantitative measurements have yet to be made. In the case of POM, two molecular weight grades have been investigated at the same drawing temperature (see Fig. 5). The effect of increasing molecular weight was to increase the degree of strain hardening whilst producing the same 10 sec modulus at a given draw ratio for each molecular weight grade. However, the long term creep behaviour of drawn POM has not yet been investigated.

6.5. Rate theory approach

The form of the flow stress–strain rate curves at constant strain levels (Figs. 4 and 5) is, in general, non-linear. It is not within the scope of the present paper to discuss in detail the implications of the observed non-linearity; this will be presented in a further publication. However, a brief discussion is appropriate. We take as our starting point the Eyring equation for an activated rate process. The plastic strain rate $\dot{\epsilon}$ is given by

$$\dot{\epsilon} = \dot{\epsilon}_0 \exp - \frac{(\Delta U - \sigma V)}{kT}$$

where

$\dot{\epsilon}_0$ is a constant
ΔU = potential energy barrier to plastic deformation
σ = applied stress
V = stress activation volume
k = Boltzmann constant
T = absolute temperature

This equation implies that the stress–ln strain rate relationship should be linear, with a slope

$$\left(\frac{\partial \sigma}{\partial \ln \dot{\epsilon}}\right)_{\epsilon} = \frac{kT}{V} = \text{constant}$$

In general this formulation is not applicable to the plastic deformation behaviour of LPE and POM.

A description of the deformation behaviour has therefore been sought in either of two possible modifications to the simple Eyring theory:

(i) two activated processes operating in parallel, each following the simple Eyring formulation, and possibly representing two physically separate processes [28, 29], or

(ii) a single activated process in which the activation volume, V, is allowed to vary with stress and/or strain [19, 20].

It appears that it is possible to describe the present data by either of these two approaches, and this will be discussed in detail in a further publication, together with its significance in relation to effective drawing. It is of interest here, however, simply to calculate values of apparent stress activation volume, V, from the slope of the stress–strain rate relationships over a wide range of strain. Where this relationship is linear, a single value of V can be obtained for the experimental stress range. Where the σ versus ln $\dot{\epsilon}$ relationship is non-linear the value of the apparent stress activation volume will change with stress level.

Fig. 13 shows that the apparent stress activation volume of R50 LPE at 100° C and D500 POM at 164° C decreases markedly from an isotropic value of several thousand cubic Ångstroms (typical for isotropic polymers [30]) to around 100 Å^3 for draw ratios greater than ~10. The latter result is in agreement with recent work in this department on the creep behaviour of drawn LPE [27]. At any fixed strain level the range of values of apparent stress activation volume (V) due to non-linearity of the σ versus ln $\dot{\epsilon}$ relationship is represented by a bar. It is not clear at present if the decrease in the apparent stress activation volume shown in Fig. 13 is directly related to the increase in strain level, or if the level of stress influences the value of V throughout the whole range of strain. It was not possible to obtain values of V at the same stress for the wide range of strain investigated; for a given experimental range of strain rate the stress range was fixed by the strain level.

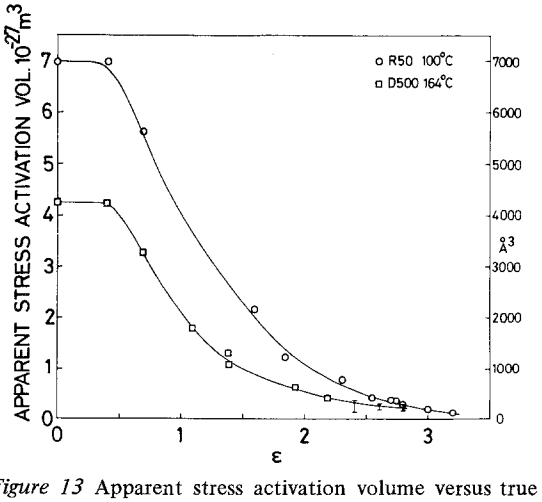

Figure 13 Apparent stress activation volume versus true strain for Rigidex 50 LPE at 100° C and Delrin 500 POM at 164° C. Bars represent the range of apparent stress activation volume observed for a range of stress at a fixed strain.

Structurally, the decrease in apparent stress activation volume observed at low draw ratios may be related to the drastic reorganization of the polymer morphology as the spherulitic structure is transformed into a fibrillar structure with increasing strain. At high draw ratios the change in apparent stress activation volume with strain is considerably smaller since the drawing then involves deformation of the fibrillar structure without large scale reorganization.

7. Conclusions

(1) It has been possible to obtain true stress–strain–strain rate data for a wide range of strain ($\epsilon = 0$ to ~3.2, $\lambda = 1$ to ~25) by combining the results of drawing isotropic and extruded samples to yield and the redrawing of fibres for Rigidex 50 LPE, Delrin 500 POM and Delrin 150 POM at elevated temperatures. The true stress–strain–strain rate surface for the given drawing temperatures was therefore determined for each polymer.

(2) The tensile flow stress of LPE and POM was found to be very strongly dependent not only upon strain but also upon strain rate, particularly at high strains. It is therefore important to account for the strain rate dependence of the flow stress in any analysis of a tensile deformation process. The paths followed across the true stress–strain–strain rate surface can be markedly different for different processes, depending upon the respective strain and strain rate fields. The cases of uniaxial tension and extrusion through convergent dies have been used to illustrate this point.

(3) Measurement of the room temperature 10 sec Young's modulus at 0.1% strain of redrawn

fibres at different draw ratios indicates that the modulus depends only upon the strain level and not upon the strain rate path followed in producing the sample, for samples of similar thermal histories.

(4) The effect of process variables such as initial morphology and molecular weight on the drawing process has been tentatively linked with the neck region in a tensile sample; the post-neck material deforms homogeneously, in a clearly defined geometrical manner, independent of initial morphology and molecular weight.

(5) A high strain hardening route of drawing appears to produce the most effective drawing in terms of enhanced properties of the product.

(6) A simple Eyring type expression does not apply in general to the plastic deformation behaviour of LPE and POM. The apparent stress activation volume of R50 LPE at 100° C changes dramatically with strain, from an isotropic value of $\sim 7000\,\text{Å}^3$ to less than $100\,\text{Å}^3$ for $\lambda > 20$. A similar fall in stress activation volume was observed for D500 POM. It is not clear at present, however, if the stress level affects the value of apparent stress activation volume throughout the whole range of strain.

(7) The true stress–strain–strain rate data can be used as a basis for a complete theoretical analysis of the hydrostatic extrusion process. A preliminary account of this has already been given [31] and more detailed discussion is to be presented in a future publication [25].

Acknowledgements

We are very much indebted to Dr R. A. Duckett for helpful discussions. PDC was supported by the Science Research Council during the course of this work.

References

1. G. CAPACCIO and I. M. WARD, *Nature Phys. Sci.* **243** (1973) 130.
2. *Idem,* British Patent Applications 10746/73, 52644/74, 52645/74, 52647/74.
3. *Idem, Polymer* **15** (1974) 233.
4. *Idem, Polymer Eng. Sci.* **15** (1975) 219.
5. *Idem, Polymer* **16** (1975) 239.
6. G. CAPACCIO, T. J. CHAPMAN and I. M. WARD, *ibid.* **16** (1975) 469.
7. J. B. SMITH, A. J. MANUEL and I. M. WARD, *ibid.* **16** (1975) 57.
8. G. CAPACCIO, T. A. CROMPTON and I. M. WARD, *J. Polymer Sci. (Phys.)* **14** (1976) 1641.
9. E. S. CLARKE and L. S. SCOTT, *ACS Polymer Prepr.* **15** (1974) 153.
10. D. L. M. CANSFIELD, G. CAPACCIO and I. M. WARD, *Polymer Eng. Sci.* **16** (1976) 721.
11. A. NADAI, "Theory of Flow and Fracture of Solids" (McGraw–Hill, New York, 1950).
12. E. OROWAN, *Rept. Prog. Phys.* **12** (1949) 185.
13. I. M. WARD, "Mechanical Properties of Solid Polymers" (John Wiley, London, 1971).
14. P. I. VINCENT, *Polymer* **1** (1960) 7.
15. *Idem,* "Physical Basis of Yield and Fracture" Institute of Physics Conference, Oxford, (1966) p.155
16. S. MARUYAMA, K. IMADA and M. TAKAYANAGI, *Int. J. Polymeric Mater.* **1** (1972) 211.
17. A. G. GIBSON and I. M. WARD, *J. Polymer Sci. (Phys.)* (to be published).
18. P. D. COATES and I. M. WARD, *ibid.* (to be published).
19. L. A. DAVIS and C. A. PAMPILLO, *J. Appl. Phys.* **42** (1971) 4659.
20. C. A. PAMPILLO and L. A. DAVIS, *ibid.* **43** (1972) 4277.
21. W. WU and A. P. L. TURNER, *J. Polymer Sci. (Phys.)* **13** (1975) 19.
22. K. NAKAMURA, K. IMADA and M. TAKAYANAGI, *Int. J. Polymeric Mater.* **2** (1972) 71.
23. K. IMADA and M. TAKAYANAGI, *ibid.* **2** (1973) 89.
24. S. MARUYAMA, K. IMADA and M. TAKAYANAGI, *ibid.* **2** (1973) 105.
25. P. D. COATES, A. G. GIBSON and I. M. WARD (to be published).
26. G. CAPACCIO, T. A. CROMPTON and I. M. WARD (to be published).
27. M. A. WILDING and I. M. WARD, *Polymer* (in press).
28. C. BAUWENS-CROWET, J. C. BAUWENS and G. HOMES, *J. Mater. Sci.* 7 (1972) 176.
29. C. BAUWENS-CROWET, *J. Mater. Sci.* 8 (1973) 968.
30. R. N. HAWARD and G. THACKRAY, *Proc. Roy. Soc.* **A302** (1968) 453.
31. A. G. GIBSON, P. D. COATES and I. M. WARD, Proceedings of the International Conference on Polymer Processing, Massachusetts Institute of Technology (1977) in press.

Received 9 December 1977 and accepted 18 January 1978.